

## Spin-Current Detection via an Interfacial Molecular Paramagnet

Thomas Marzi,<sup>1</sup> Ralf Meckenstock,<sup>1</sup> Sabrina Masur,<sup>2</sup> and Michael Farle<sup>1,\*</sup>

<sup>1</sup>AG Farle, Faculty of Physics and Center for Nanointegration (CeNIDE), University of Duisburg-Essen, Lotharstraße 1, 47048 Duisburg, Germany

<sup>2</sup>Cavendish Laboratory, Department of Physics, JJ Thomson Avenue, Cambridge CB3 0HE, United Kingdom



(Received 22 September 2016; revised manuscript received 2 October 2018; published 1 November 2018)

Pure spin currents are considered as key processes for future low-dissipation electronics. Current detection schemes use the inverse spin Hall effect for converting the spin current into an electrical voltage. Here we present an alternative, contact-free detection scheme based on a paramagnetic molecular probe layer that in principle allows the integration of spin currents into molecular electronics. In a measurement without the requirement of lithographically tailored samples and electrical contacts, we detect changes of the electron spin resonance in the probe layer when a spin current is injected from a microwave-driven ferromagnetic layer. Tuning the microwave resonance conditions of the ferromagnetic and molecular layer to the same resonance condition, we observe the flow of spin momentum at the interface through the change of the microwave-power-dependent absorption of the adsorbed molecular layer. We use oleic acid as the molecular probe layer on metallic and oxidized iron films.

DOI: 10.1103/PhysRevApplied.10.054002

### I. INTRODUCTION

For the design of future magnetologic storage devices and integrated circuits, it is of utmost importance to understand the properties and interactions of spin currents at interfaces between different materials. Furthermore, it is imperative to sensitively detect spin currents for subsequent processing of information. Two types of spin current are distinguished: (a) “conduction-electron spin current,” where the spin angular momentum is carried by electron diffusion; (b) “spin-wave spin current,” where the spin angular momentum is carried by a collective precession of magnetic moments [1]. Diffusive spin currents were discussed by Silsbee and coworkers [2,3] as a “transport of magnetization” across a ferromagnetic/paramagnetic metal interface that is detected by changes of the conduction electron spin resonance (ESR) in a thin layer of Cu interfaced with permalloy. Their model was based on a phenomenological exchange coupling of *d* electrons to the *s* electrons traveling across the interface in both directions. Later the model of pure spin currents (i.e., flow of spin angular momentum while no net charge transport occurs) was developed, and the effects of spin currents in paramagnetic metal layers were measured by the inverse spin Hall effect [4–6]. The latter typically requires lithographically prepared and electrically contacted samples as well as metallic or semiconducting detection layers for the conversion of the spin current into an electrical voltage.

Here we propose an alternative method [Fig. 1(a)] to detect pure spin currents by detecting changes of the amplitude of ESR of a paramagnetic molecular probe layer. In our prototype experiment we use oleic acid (OA) [Fig. 1(b)] deposited on ferromagnetic Fe and initiate the spin-pumping process by precessing the Fe magnetization in a microwave field. The method is noninvasive since electrical contacts are not necessary, and it does not rely on the detection of small voltages that are prone to artifacts. As a side note, we mention that this detection scheme can also be used as a nanothermometer to measure temperature changes directly at the metal/paramagnet interface (e.g., the surface temperature of colloidal nanoparticles [7] in biomedical hyperthermia).

### II. EXPERIMENTAL SECTION

#### A. Sample preparation and characterization

A  $4 \times 4$  mm<sup>2</sup> GaAs(100) substrate is heated in an ultrahigh-vacuum (UHV) chamber with a base pressure of  $6 \times 10^{-11}$  mbar to 900 K while being sputtered with argon ions at a partial pressure  $p_{\text{Ar}} = 1.5 \times 10^{-5}$  mbar. Subsequently, the substrate is annealed at 900 K for 30 min, resulting in a {4 × 6} surface-reconstructed GaAs surface. Then 4–7-nm-thick epitaxial (001) iron films are deposited by electron-beam evaporation at a rate of 0.7 Å/min [8]. The crystallinity and contamination levels are monitored by low-energy electron diffraction (LEED) and Auger electron spectroscopy (AES). The cleaned GaAs(001) shows

\*farle@uni-due.de

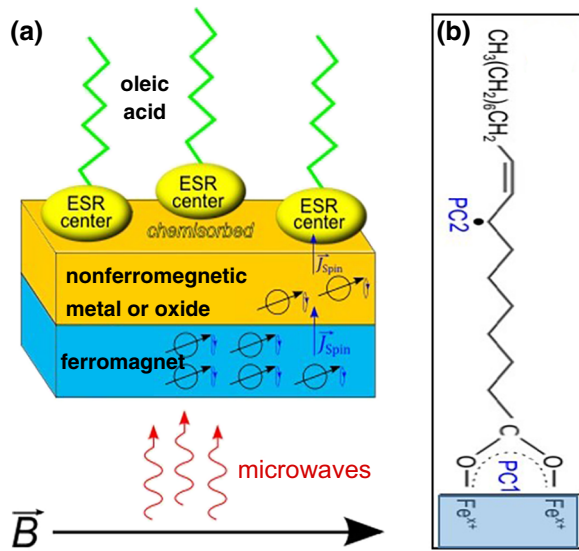


FIG. 1. (a) Concept of spin-current detection by a chemisorbed molecular paramagnetic probe (ESR center) such as oleic acid. The magnetization of the ferromagnet is resonantly excited by microwaves in an external magnetic field  $\vec{B}$ , and a spin current travels across the interface into the monolayer of paramagnetic molecules. The paramagnetic monolayer can be separated by a nonferromagnetic metal or insulator with variable thickness from the ferromagnet. (b) Molecular structure and bonding of oleic acid on Fe with the carboxyl end group. PC1 and PC2 indicate ESR centers that are detected.

the typical stripe LEED pattern. With subsequent Fe coverage, the GaAs pattern vanishes, and a weak Fe pattern is observed. OA is evaporated from a carefully rinsed and evacuated glass nozzle located near the Fe film at 313 K. After adsorption of OA, no LEED pattern is observed. Characteristic Auger spectra for different stages of adsorption of OA on Fe are shown in Fig. 2; that is, for the uncovered, freshly prepared 7-nm Fe film (blue) and for the same Fe film after exposure to 600 l O<sub>2</sub> (red) at 300 K and subsequent exposure to 15 l OA (green). As expected, a distinct oxygen peak is recorded after surface oxidation (red spectrum) and a pronounced C signal at 273 eV is recorded after exposure to OA. The inset in Fig. 2 shows a magnification of the energy range of the MVV transition (47 eV) of iron. The red spectrum reveals the formation of Fe<sub>2</sub>O<sub>3</sub> characterized by Auger transitions at 43 and 51 eV. This is accompanied by a considerable drop of intensity. When the oxidized iron film is exposed to 15 l oleic acid, the signal intensity at 43 eV is again drastically reduced.

*In situ* ESR and ferromagnetic resonance (FMR) measurements are performed on Fe films after exposure to only few langmuirs of OA. Subsequently, angular- and temperature-dependent ESR and ferromagnetic resonance (FMR) measurements at X-band frequencies are performed *in situ* and *ex situ* as described below. Fe films for *ex situ* ESR and FMR experiments are removed from the

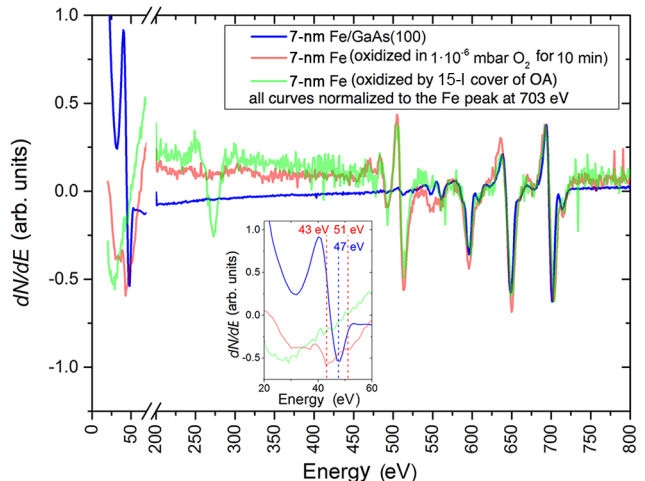


FIG. 2. Auger spectra of Fe films after exposure to OA. Three different spectra normalized to the iron peak at 703 eV after different exposures to oxygen and OA are shown.

UHV chamber, oxidized in laboratory air, and covered with 1  $\mu$ l OA.

## B. Chemisorption of oleic acid on iron

OA, which is a carboxylic acid [C<sub>18</sub>H<sub>34</sub>O<sub>2</sub>; Fig. 1(b)], is routinely used in colloidal synthesis of nanoparticles to control and stabilize their size and shape as well as for prevention of agglomeration [9–11]. During chemisorption of OA on an oxidized Fe surface, the oleic acid's carboxylic group (COOH) converts to carboxylate (COO<sup>-</sup>) by releasing the hydroxyl's proton [see Fig. 1(b)]. The oxygen atoms are coordinated symmetrically to the iron oxide surface [11,12], while the carboxylate's extra electron remains delocalized, forming an ESR center. Neither the pure iron film nor the pure oleic acid molecules generate an ESR signal. After chemisorption, an ESR signal with a *g* factor of  $2.004 \pm 0.001$  is observed. The origin of the ESR signal is attributed to a partial charge transfer of the chemisorbed OA molecule to Fe, resulting in a paramagnetic center (PC1) directly at the interface [Fig. 1(b)]. The paramagnetic center (PC1) detected in our experiment is a partially delocalized electron of the carboxyl group of OA. A second ESR signal [PC2 in Fig. 1(b)] could result from an unpaired electron when the double bond at PC2 is broken. This, however, has been observed only after the organometallic synthesis of Fe particles when OA is used as a stabilizer (see, e.g., Ref. [7]) at temperatures much higher than room temperature. The ESR signal (either PC1 or PC2) as a paramagnetic spin moment is independent of the angle between the sample plane and the external magnetic field, and it can be used as a local probe for spin currents, spin-polarized current, or temperature changes at the interface with atomic resolution. For example, the sensitivity to temperature was

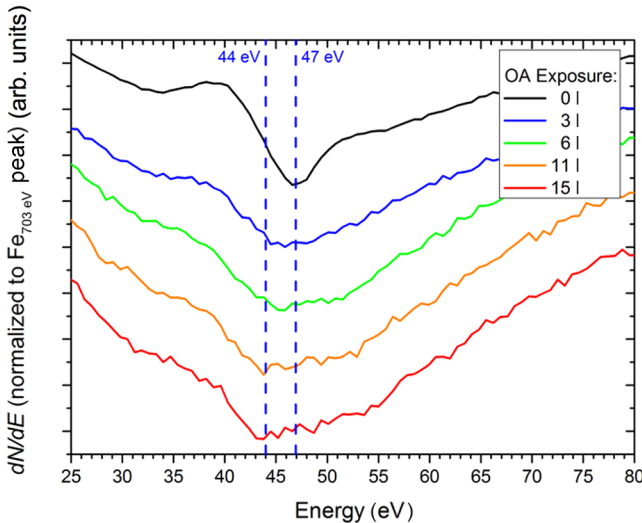


FIG. 3. High-resolution Fe (MNN) Auger spectra recorded in situ in UHV with different exposures (1 := Langmuir = 1 torr  $\mu$ s) to oleic acid.

demonstrated earlier for magnetic nanoparticles [7], where we analyzed the nanoparticle heating due to microwave absorption noninvasively.

To confirm the chemical character of the ESR signal discussed below, high-resolution Fe (47 eV) Auger spectra were recorded (Fig. 3). The clean iron surface (black spectrum in Fig. 3) is exposed to 0–15 L OA (1 := Langmuir) in steps of 0.25 L. At 11 L, the Fe signal shifts to 44 eV (orange curve), which was previously ascribed to the formation of  $Fe^{3+}$  in  $Fe_2O_3$  [13–15]. The decrease of the signal-to noise ratio is due to screening of the low-energy electrons [15] by OA. This result suggests that OA creates an  $Fe^{3+}$  state on the iron surface. Moreover, formation of  $FeO$  or  $Fe_3O_4$  can be excluded, since the peak at 44 eV can be assigned only to  $Fe_2O_3$  [14,15]. Further addition of OA does not yield any additional changes in the Fe Auger spectrum (red spectrum for 15 L), and yields the expected signal at 273 eV for the carbon in oleic acid (Fig. 2).

### C. Electron spin resonance of adsorbed oleic acid

The *in situ* UHV ESR spectra are recorded with a Varian cylindrical cavity at  $f = 9.21$  GHz in an UHV quartz tube setup as described earlier. The *ex situ* ESR measurements are performed at X-band frequency  $f = 9.68$  GHz in a Bruker cylindrical cavity [16]. All magnetic resonance spectra are recorded with a standard field-modulation technique at 100 kHz and a modulation amplitude at least 5 times smaller than the linewidth of the ESR resonances. The *in situ* ESR for different OA coverage shows that a slight oxidation of the epitaxial Fe surface is required to detect an ESR signal at the interface. Figure 4 shows a comparison of the ESR signals after exposure of a clean and preoxidized Fe film to 10 L OA. The ESR signal of the

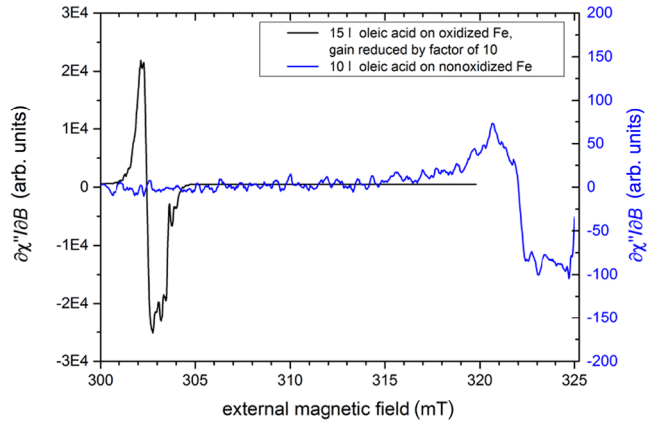


FIG. 4. *In situ* ESR spectra of 7-nm Fe covered with OA (blue, right axis) and another 7-nm preoxidized Fe film covered with OA (black, left axis). Note the orders-of-magnitude increase of the OA signal and decrease of linewidth on the oxidized surface indicating a lower relaxation rate.

Fe film preoxidized in 600 L  $O_2$  and subsequently exposed to 15 L OA is about 200 times larger in amplitude (black spectrum, left axis in Fig. 4). Since the degree of oxidation of the iron surface before application of OA correlates with the amplitude of the ESR signal, we conclude that oxidation of the iron surface is required for the chemisorption of OA and thus the appearance of the ESR signal. ESR and FMR measurements on  $Fe/Fe_xO_y$  core-shell nanoparticles synthesized with OA have shown an additional ESR signal that could be clearly identified as resulting from the break of a double bond [PC2 in Fig. 1(b)] in OA [7]. This is not the case in the chemisorption of OA on the pure Fe surface studied in an UHV here.

In our UHV experiments, we observe that during the acquisition of several spectra the resonance field changes by 5 mT. After shutting off the previously applied microwave power of 20 mW for about 5 h and then measuring again using 20 mW, we find the resonance field has returned to its original value. In addition, the signal-to-noise ratio decreases. Both findings confirm a rise of temperature during the measurement, which was also observed in a comparable paramagnetic nanoparticle system [7].

## III. RESULTS AND DISCUSSION

As the resonant spin excitation in the ferromagnetic Fe film causes a pure spin current [6,17,18] across the interface, this additional local high spin polarization modifies the occupation of the Zeeman-split energy levels of the paramagnetic molecule at the interface (additional excitations). This change is observed as a variation of the ESR amplitude but not the linewidth. One may compare our observations with previous conduction-ESR experiments in metallic Cu and Ag films in contact with a ferromagnetic layer where changes of the relaxation rate of the

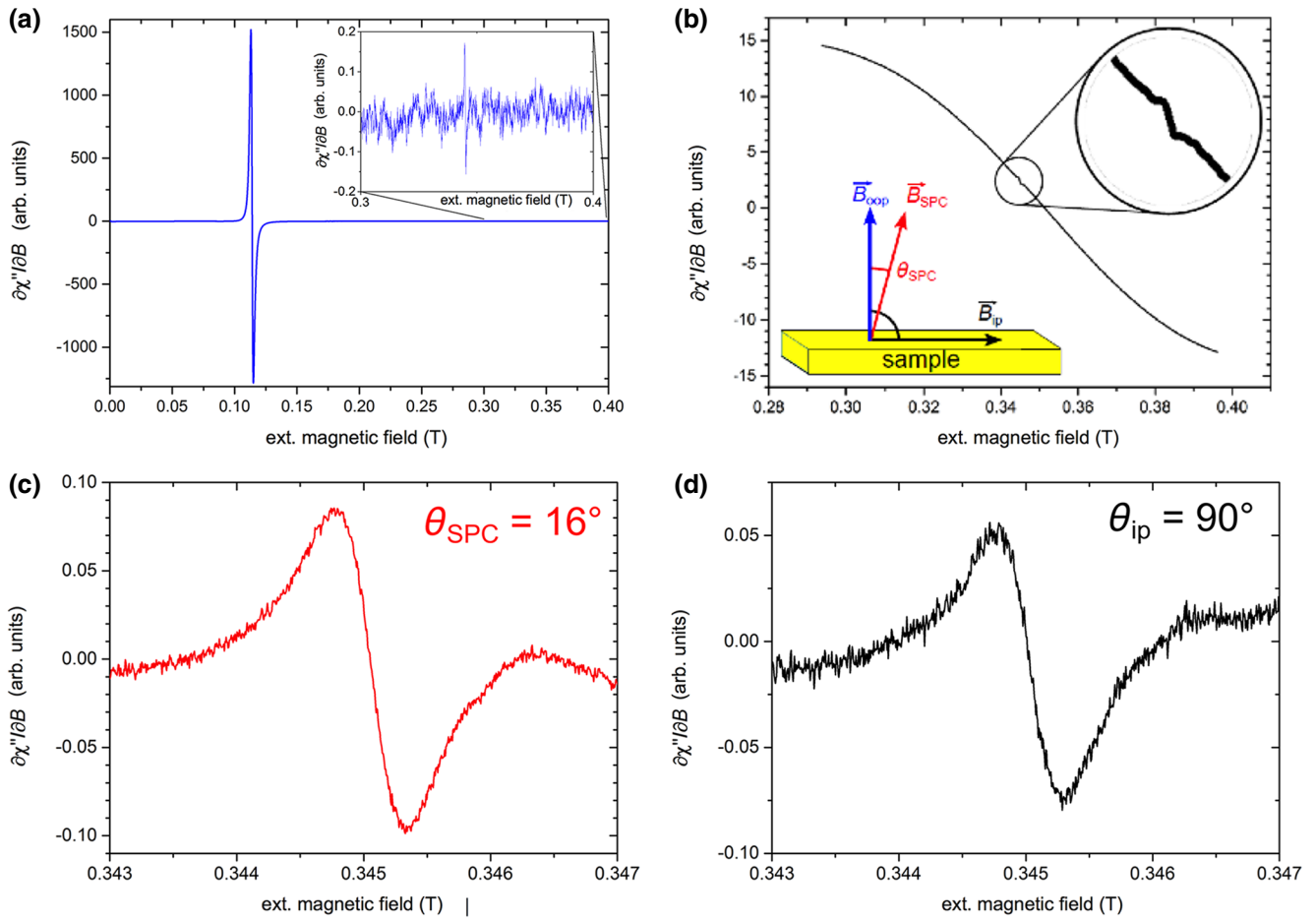


FIG. 5. (a) *Ex situ* spectrum of oleic acid on a single-crystal Fe film with the magnetic field oriented at  $\theta_{ip} = 90^\circ$ , where the FMR and ESR (inset) signals are well separated. (b) *Ex situ* spectrum of oleic acid on a polycrystalline 9-nm Fe film in the spin-pumping configuration ( $\theta_{SPC} = 15.5^\circ$ ), where the Fe FMR and the OA ESR occur at the same resonance field  $B_R$ . (c) ESR signal after background subtraction of Fe signal. (d) EPR signal in (a) that is non-spin-pumping configuration (IP = in-plane).

delocalized conduction-electron spins were detected and interpreted as a coupling of the spins diffusing (called “magnetization transport” in Ref. [2]) from the ferromagnetic metal into the nonferromagnetic metal film [3,17]. This model is very reminiscent of the current spin-pumping models, but has been mostly neglected in recent literature. The ESR of a localized paramagnetic molecular surface monolayer—such as OA—is, however, different. While tuning the FMR and ESR resonance condition of both layers to the same frequency, one can follow the influence of pure spin currents emitted by the collective magnetization precession in the ferromagnetic layer on the quantum mechanical excitation of the paramagnetic spins of the probe layer. The flow of spin momentum is reflected in the microwave-power-dependent absorption characteristics of the ESR directly measured at the interface. In other words, the ESR signal results from a localized molecular site, and the spin torque exerted by the spin imbalance of conduction electrons in the spin-pump models can be interpreted as scattering events in the Zeeman-split spin-up

and spin-down levels of the molecular complex, thereby changing their occupation numbers and accordingly the intensity of the ESR signal.

The well-known angular dependence of the FMR of the Fe film (see, e.g., Ref. [19]) allows us to identify and set the angle between the Fe-film plane and the external magnetic field in such a way that the “spin-pumping” FMR line position of the iron film coincides with the angular-independent ESR line position of OA. Because of their independent excitation processes, the two modes do not couple to each other. We call this configuration a “spin-pumping configuration” (SPC), and the corresponding angle of the external magnetic field is  $\theta_{SPC}$ . A complete angular dependence from in plane  $\theta_{ip} = 90^\circ$  to out of plane  $\theta_{oop} = 0^\circ$  is measured to determine the magnetic properties of the Fe film and to confirm the angle independence of the ESR signal. Exemplary microwave-absorption spectra are shown in Fig. 5 for two orientations: The external field  $B$  is oriented in the film plane, where the FMR of the Fe film at  $B_R^{Fe}(\theta_{ip}) = 120$  mT is well separated from the OA

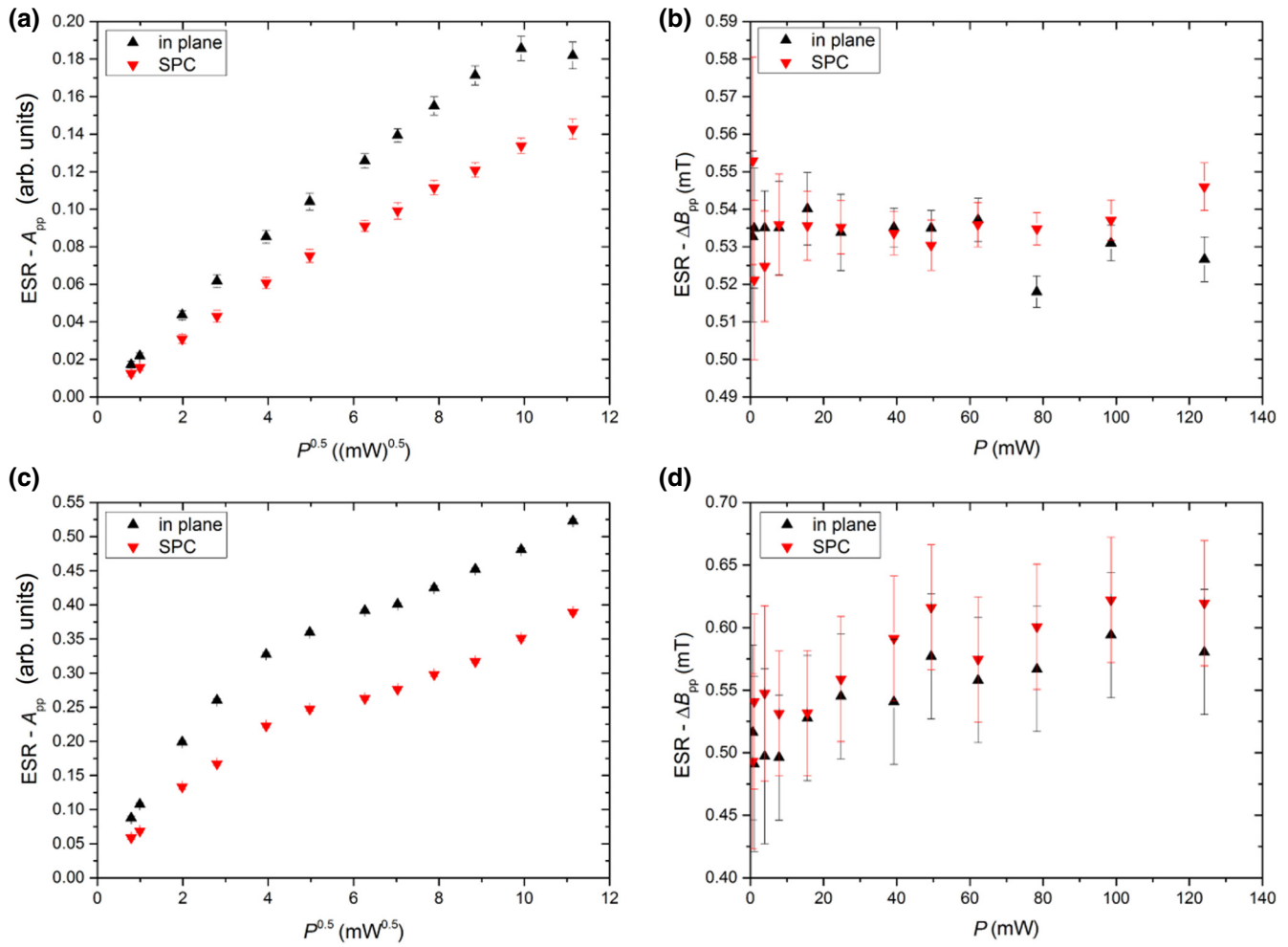


FIG. 6. Results of *ex situ* experiments at  $\theta_{\text{oop}} = 90^\circ$  (black) and in the SPC (red): the peak-to-peak ESR amplitude  $A_{\text{pp}}$  (a),(c) and linewidth  $\Delta B_{\text{pp}}$  (b),(d) of OA as a function of microwave power on an oxidized polycrystalline Fe film and on a single-crystal Fe film, respectively.

ESR ( $B_R^{\text{OA}} = 345$  mT) [Fig. 5(a)]. The sample is rotated to  $\theta_{\text{SPC}}$  and ESR and FMR occur at the same resonance field  $B_R^{\text{Fe}} = B_R^{\text{OA}}$  [Fig. 5(b)]. The inset in Fig. 5(b) illustrates the different angles with respect to the sample plane, and the ESR line on the much stronger Fe FMR background signal is magnified in the circle.

In the following we discuss the ESR spectra of OA adsorbed on 4- and 5-nm Fe films recorded at different microwave powers between 0.6 and 124 mW for  $\theta_{\text{ip}} = 90^\circ$  and  $\theta_{\text{SPC}}$ . In the case of the SPC, the broad and strong FMR Fe “background” signal is subtracted to get the pure ESR contribution [Fig. 5(c)]. For comparison, the signal in the in-plane configuration is shown in Fig. 5(d). The peak-to-peak amplitude  $A_{\text{pp}}$  and linewidth  $\Delta B_{\text{pp}}$  of the ESR signals of in-plane and SPC measurements are plotted versus the applied microwave power in Fig. 6.

The ESR amplitude [Fig. 6(a)] linearly increases with the square root of the microwave power as expected for unsaturated microwave absorption. It is important to mention that this behavior—“one photon is flipping one

spin”—is valid only for ESR and not for collective excitation of FMR. The slope of the ESR amplitude for the  $\theta_{\text{SPC}}$  configuration [red in Fig. 6(a)] is significantly smaller than in the  $\theta_{\text{ip}}$  configuration [black in Fig. 6(a)]. In addition, the linewidth [Fig. 6(b)] does not reveal any significant differences within the error bars for increasing excitation power and the two angular configurations. The origin of the amplitude change between the two orientations is due to additional excitation by the spin current of the ferromagnet resulting in a higher average occupation of the upper Zeeman level. Within the resolution of the experiment, the lifetime of the microwave-excited ESR state, which is proportional to the linewidth of the resonance, does not change. Thus, the spin current at the interface (iron/OA) coherently excites additional paramagnetic spins in the OA interface layer and reduces the difference of the occupation number of up and down states, yielding a decrease of the absorption amplitude in the SPC relative to the in-plane or out-of-plane configuration. Theoretically, an influence of the spin current on the lifetime of the excited spins could

be expected. This, however, is too small to be detected due to the phase coherence of the spin current.

The results of the ESR measurements of OA on the single-crystal iron film are shown in Figs. 6(c) and 6(d). We find the same characteristic differences for the power dependence of the ESR amplitude [Fig. 6(c)] as in the case of the polycrystalline film. The measured amplitude is larger for the in-plane configuration than for the SPC. Only the slope of the amplitude changes at a microwave power of about 16 mW for both orientations. Thus, it is an effect independent of the SPC condition and might be due to the lower surface roughness of the (001) interface of the epitaxial film compared with the polycrystalline film. Therefore, the adsorption sites of OA are fewer and more uniform. This, in turn, leads to a generally-better-defined equilibrium of up and down states, yielding a saturation of the ESR amplitude at lower powers compared with the polycrystalline film [Fig. 6(a)]. The much-better-defined epitaxial interface seems to result in a slightly higher relaxation rate (larger linewidth) in the SPC. However, we cannot unambiguously quantify this difference within the experimental error [Fig. 6(d)].

#### IV. CONCLUSION

Atomically resolved spin-pumping effects at the surface of ferromagnetic Fe are detected by the change of occupation of spin-up and spin-down states in a paramagnetic molecule adsorbed at the surface. We find that within the resolution of the technique, the lifetime of the excited Zeeman level in the paramagnet is not modified by the spin current. This contact-free method can be extended to other paramagnetic adsorbates and may find applications in molecular electronics. Additional nonferromagnetic spacer layers can be introduced to tune the strengths of the momentum transfer and the diffusion length of spin currents.

#### ACKNOWLEDGMENTS

We thank K. Wagner, F.M. Römer, and S. Liébana Viñas for valuable discussions. Financial support by the DFG (SPP 1538 Spin Caloric Transport) is acknowledged.

- 
- [1] K.-i. Uchida, H. Adachi, Y. Kajiwara, S. Maekawa, and E. Saitoh, *Spin-Wave Spin Current in Magnetic Insulators*, in *Recent Advances in Magnetic Insulators – From Spintronics to Microwave Applications* (Elsevier, 2013), p. 1.
  - [2] P. D. Sparks and R. H. Silsbee, Magnetization transport across a ferromagnetic-paramagnetic interface, *Phys. Rev. B* **35**, 5198 (1987).
  - [3] R. H. Silsbee, A. Janossy, and P. Monod, Coupling between ferromagnetic and conduction-spin-resonance modes at a ferromagnetic-normal-metal interface, *Phys. Rev. B* **19**, 4382 (1979).
  - [4] E. Saitoh, M. Ueda, H. Miyajima, and G. Tatara, Conversion of spin current into charge current at room temperature: Inverse spin-Hall effect, *Appl. Phys. Lett.* **88**, 182509 (2006).
  - [5] M. Weiler, M. Althammer, M. Schreier, J. Lotze, M. Pernpeintner, S. Meyer, H. Huebl, R. Gross, A. Kamra, J. Xiao, Y. T. Chen, H. Jiao, G. E. Bauer, and S. T. Goennenwein, Experimental Test of the Spin Mixing Interface Conductivity Concept, *Phys. Rev. Lett.* **111**, 176601 (2013).
  - [6] P. C. Lou and S. Kumar, Generation and detection of dissipationless spin current in a MgO/Si bilayer, *J. Phys.: Condens. Matter* **30**, 145801 (2018).
  - [7] S. Masur, B. Zingsem, T. Marzi, R. Meckenstock, and M. Farle, Characterization of the oleic acid/iron oxide nanoparticle interface by magnetic resonance, *J. Magn. Magn. Mater.* **415**, 8 (2016).
  - [8] K. Zakeri, T. Kebe, J. Lindner, and M. Farle, Correlation between structure and magnetism in epitaxial Fe monolayers on GaAs(001), *Superlattices Microstruct.* **41**, 116 (2007).
  - [9] M. V. Kovalenko, M. I. Bodnarchuk, R. T. Lechner, G. Hesser, F. Schäffler, and W. Heiss, Fatty acid salts as stabilizers in size- and shape-controlled nanocrystal synthesis: The case of inverse spinel iron oxide, *J. Am. Chem. Soc.* **129**, 6352 (2007).
  - [10] W. Wu, Q. He, and C. Jiang, Magnetic iron oxide nanoparticles: synthesis and surface functionalization strategies, *Nanoscale Res. Lett.* **3**, 397 (2008).
  - [11] L. Zhang, R. He, and H.-C. Gu, Oleic acid coating on the monodisperse magnetite nanoparticles, *Appl. Surf. Sci.* **253**, 2611 (2006).
  - [12] A. Drmota, A. Kosak, and A. Znidarsic, A mechanism for the adsorption of carboxylic acids onto the surface of magnetic nanoparticles, *Mater. Technol.* **42**, 79 (2008).
  - [13] T. Kebe, K. Zakeri, J. Lindner, M. Spasova, and M. Farle, Magnetization and magnetic anisotropy energy of ultra-thin Fe films on GaAs(001) exposed to oxygen, *J. Phys.: Condens. Matter* **18**, 8791 (2006).
  - [14] V. S. Smentkowski and J. T. Yates, The adsorption of oxygen on Fe(110) in the temperature-range of 90-K to 920-K, *Surf. Sci.* **232**, 113 (1990).
  - [15] M. Seo, J. B. Lumsden, and R. W. Staehle, An AES analysis of oxide films on iron, *Surf. Sci.* **50**, 541 (1975).
  - [16] M. Farle, M. Zomack, and K. Baberschke, Electron-spin-resonance of adsorbates on single-crystal metal-surfaces under UHV conditions, *Surf. Sci.* **160**, 205 (1985).
  - [17] A. Brataas, Y. Tserkovnyak, G. E. W. Bauer, and B. I. Halperin, Spin battery operated by ferromagnetic resonance, *Phys. Rev. B* **66**, 060404 (2002).
  - [18] Y. Tserkovnyak, A. Brataas, and G. E. W. Bauer, Enhanced Gilbert Damping in Thin Ferromagnetic Films, *Phys. Rev. Lett.* **88**, 117601 (2002).
  - [19] F. M. Römer, C. Hassel, K. Zakeri, C. Tomaz, I. Barsukov, R. Meckenstock, J. Lindner, and M. Farle, Fe monolayers on InAs(001): An in situ study of surface, interface and volume magnetic anisotropy, *J. Magn. Magn. Mater.* **321**, 2232 (2009).